

Communication

A Redox Strategy for Light-Driven, Out-of-Equilibrium Isomerizations and Application to Catalytic C–C Bond Cleavage Reactions

Eisuke Ota, Huaiju Wang, Nils Lennart Frye, and Robert R Knowles

J. Am. Chem. Soc., **Just Accepted Manuscript** • DOI: 10.1021/jacs.8b12552 • Publication Date (Web): 10 Jan 2019

Downloaded from <http://pubs.acs.org> on January 10, 2019

Just Accepted

“Just Accepted” manuscripts have been peer-reviewed and accepted for publication. They are posted online prior to technical editing, formatting for publication and author proofing. The American Chemical Society provides “Just Accepted” as a service to the research community to expedite the dissemination of scientific material as soon as possible after acceptance. “Just Accepted” manuscripts appear in full in PDF format accompanied by an HTML abstract. “Just Accepted” manuscripts have been fully peer reviewed, but should not be considered the official version of record. They are citable by the Digital Object Identifier (DOI®). “Just Accepted” is an optional service offered to authors. Therefore, the “Just Accepted” Web site may not include all articles that will be published in the journal. After a manuscript is technically edited and formatted, it will be removed from the “Just Accepted” Web site and published as an ASAP article. Note that technical editing may introduce minor changes to the manuscript text and/or graphics which could affect content, and all legal disclaimers and ethical guidelines that apply to the journal pertain. ACS cannot be held responsible for errors or consequences arising from the use of information contained in these “Just Accepted” manuscripts.

A Redox Strategy for Light-Driven, Out-of-Equilibrium Isomerizations and Application to Catalytic C–C Bond Cleavage Reactions

Eisuke Ota, Huaiju Wang, Nils Lennart Frye, and Robert R. Knowles*

Department of Chemistry, Princeton University, Princeton, NJ 08544, United States

Supporting Information Placeholder

ABSTRACT: We report a general protocol for the light-driven isomerization of cyclic aliphatic alcohols to linear carbonyl compounds. These reactions proceed via proton-coupled electron transfer (PCET) activation of alcohol O–H bonds followed by subsequent C–C β -scission of the resulting alkoxy radical intermediates. In many cases, these redox-neutral isomerizations proceed in opposition to a significant energetic gradient, yielding products that are less thermodynamically stable than the starting materials. A mechanism is presented to rationalize this out-of-equilibrium behavior that may serve as a model for the design of other contrathermodynamic transformations driven by excited-state redox events.

Thermal isomerizations play a key role in synthetic chemistry, reorganizing the bonds in accessible substrates to furnish more valuable (and thermodynamically stable) products.¹ In contrast, methods that enable isomerizations to proceed “uphill” against an energetic gradient are less common and present an interesting challenge in reaction design. Being redox-neutral by definition, unimolecular isomerizations generally do not permit the incorporation or removal of substituents by reaction with stoichiometric reagents, excluding a source of driving force accessible in most other reaction types.² Moreover, once formed, the desired higher-energy isomer must be kinetically isolated from conversion back to the more stable starting material during the course of the reaction.

Photochemical approaches are commonly employed to overcome these constraints, and photo-driven out-of-equilibrium isomerizations have been extensively studied.^{3,4} While these reactions are generally understood to proceed via electronic excited states of the substrates undergoing isomerization, in principle any reaction sequence that proceeds on two distinct potential surfaces can break detailed balance and be driven away from thermal equilibrium.⁵ Accordingly, we have recently become interested in developing general, light-driven strategies for achieving out-of-equilibrium transformations that operate through excited-state redox events.

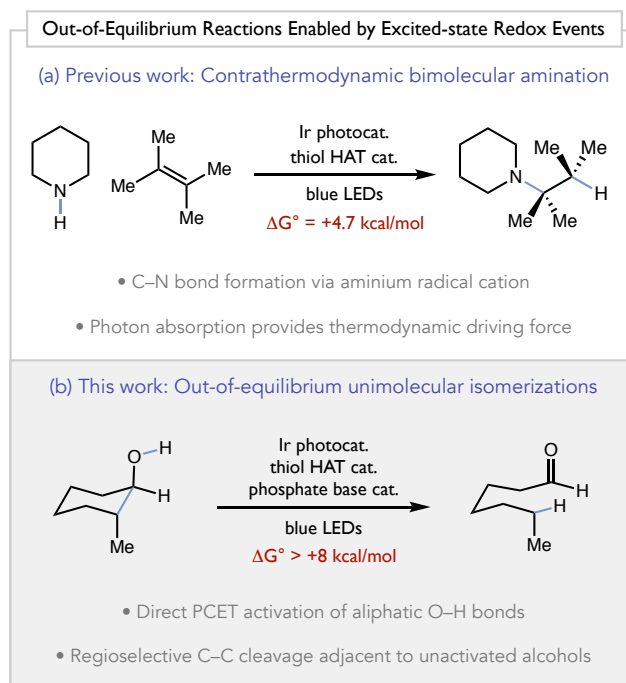
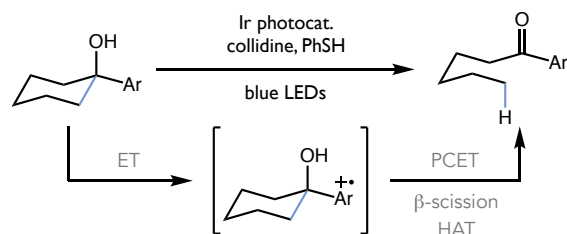


Figure 1. Catalysis out of equilibrium: (a) intermolecular anti-Markovnikov hydroamination (b) PCET-based isomerizations of aliphatic alcohols.

These electron transfer-based approaches provide a complementary mechanism for selectively channeling the energy from photon-absorption events to drive reactions in opposition to a thermodynamic bias. However, they are potentially applicable to a wider range of substrates and reaction types than direct excitation or energy transfer-based approaches. In line with these goals, we recently reported a photoredox protocol for intermolecular anti-Markovnikov hydroamination where certain 3° amine products were shown to be less stable than their constituent olefin and 2° amine starting materials (Figure 1A).⁶ Building on these results, we report here a significantly improved light-driven method for the contrathermodynamic isomerization of cyclic aliphatic alcohols and hemiacetals to linear carbonyl compounds (Figure 1B). While these redox-neutral isomerizations proceed irreversibly and in high yield, in many examples

the carbonyl-containing products are thermodynamically less stable than the alcohol starting materials. We propose that this non-equilibrium stationary state is driven by the action of excited-state proton-coupled electron transfer (PCET) events and maintained through a ratchet-type mechanism, similar to those invoked to describe the out-of-equilibrium behavior in molecular machines and motors.^{7,8} The optimization, scope studies, and mechanistic discussion of this process are presented herein.

This work finds its basis in a previous report from our laboratory describing catalytic alkoxy radical generation based on the multi-site proton-coupled electron transfer activation of a cyclic alcohol O–H bond followed by a subsequent C–C bond β -scission to cleave a carbocyclic ring.^{9,10} Our initial report outlined a photocatalytic method incorporating these elementary steps that functioned to isomerize a wide range of cyclic tertiary benzylic alcohols to linear aryl ketone products. However, this protocol relied on a redox-relay strategy wherein oxidation of a substrate-based aromatic group by the excited state Ir photocatalyst generates an arene radical cation intermediate that can serve as the internal oxidant for the PCET activation of a proximal alcohol O–H bond (Figure 2).¹¹ Consequently, simple aliphatic alcohols lacking an oxidizable arene were not viable substrates for this method.



Prior method: requirement for arene radical-cation redox relay

Figure 2. Prior PCET method requires a tertiary benzylic alcohol substrate with an oxidizable arene.

Seeking to overcome this limitation, we set out to develop a more general method that would both enable direct PCET-based homolytic activation of the O–H bonds in 1°, 2°, and 3° aliphatic alcohols and hemiacetals and successfully mediate the subsequent β -scission reactions of the resulting alkoxy radicals.^{12,13} Our initial attempts focused on the catalytic isomerization of cyclic glucose derivative **1** to linear formate **1a**.¹⁴ Notably, the optimized conditions from our previous report on the isomerization of tertiary benzylic alcohols, which made use of [Ir(dF(CF₃)ppy)₂(5,5'-d(CF₃)bpy)]PF₆ (**Ir**), collidine base, thiophenol H-atom donor, and dichloromethane solvent proved unsuccessful, providing the desired product in only 6% yield after irradiation with blue LEDs at room temperature (Table 1, entry 1). Changing the solvent to toluene and the thiol to 2,4,6-triisopropyl

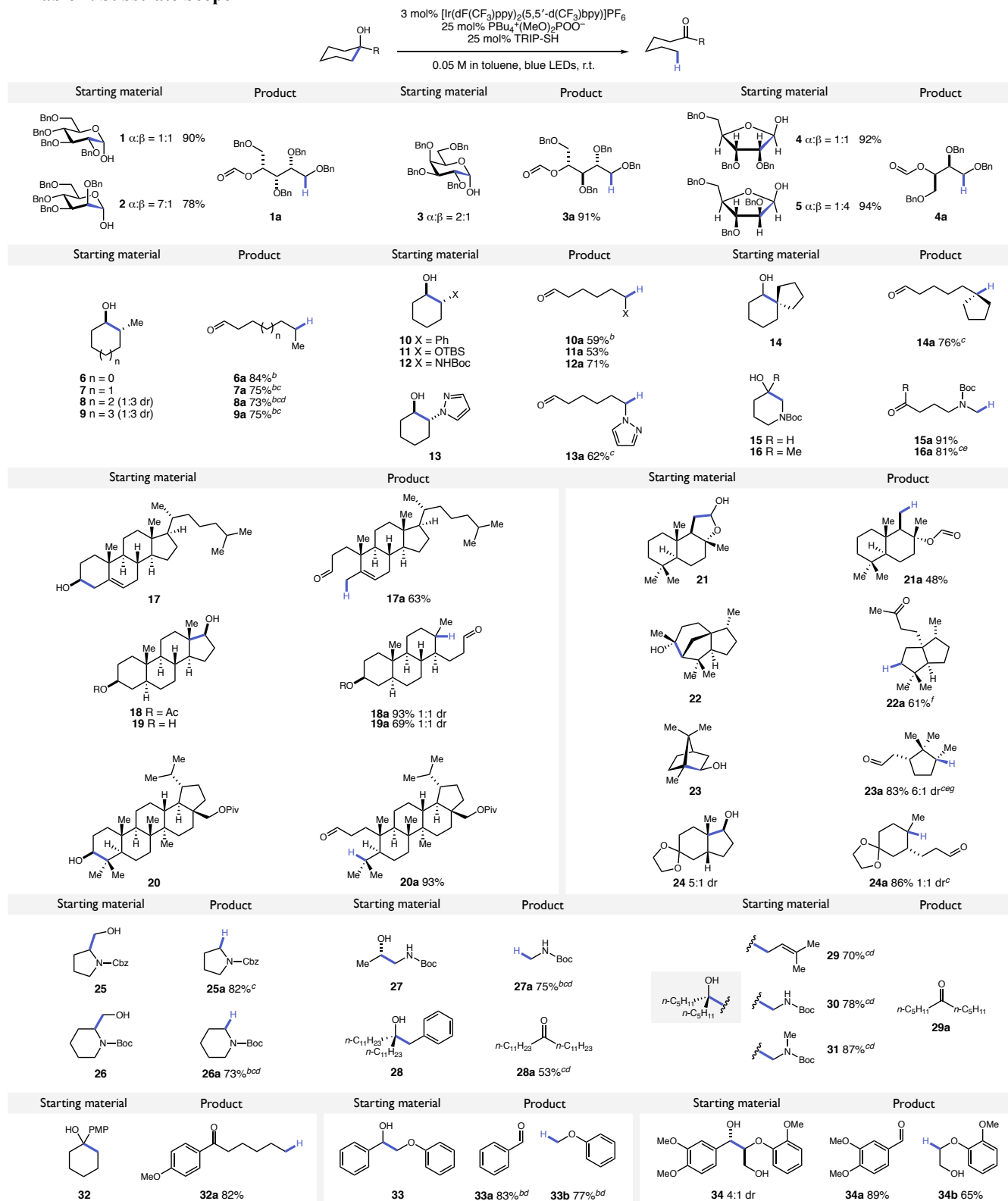
benzenethiol (TRIP-SH) modestly improved the reactivity (entry 2). Substitution of the neutral collidine base for the anionic tetrabutylammonium diphenyl phosphate gave a more significant increase, providing **1a** in 69% yield (entry 3). We speculate that this outcome may result from the propensity of the anionic phosphate base to form a more favorable hydrogen bond complex with the alcohol substrate, a key mechanistic requirement for PCET activation. Further optimization of the phosphate structure revealed that alkyl substituents were more effective than the phenyl derivative, with tetrabutylammonium dibutyl phosphate providing **1a** in 79% yield (entry 4). Next, we observed that the exchange of the alkyl ammonium cation with the corresponding alkyl phosphonium led to further improvements in reaction efficiency (entry 5). Finally, we found that tetrabutylphosphonium dimethyl phosphate was the optimal base in this process, providing the desired ring opened product **1a** in essentially quantitative yield (entry 6) after 24 hours of blue LED irradiation at room temperature. Control reactions conducted in the absence of photocatalyst, base, thiol, or visible light irradiation resulted in complete loss of reactivity, indicating the essential role of each component (entries 7–10).

Table 1. Reaction Optimization^a

Entry	Conditions	Yields (%)
1	2,4,6-collidine (3 eq.), PhSH (0.25 eq.), CH ₂ Cl ₂ solvent	6
2	2,4,6-collidine (0.25 eq.)	19
3	NBu ₄ ⁺ (PhO) ₂ POO ⁻	69
4	NBu ₄ ⁺ (<i>n</i> -BuO) ₂ POO ⁻	79
5	PBu ₄ ⁺ (<i>n</i> -BuO) ₂ POO ⁻	87
6	PBu ₄ ⁺ (MeO) ₂ POO ⁻	99
<i>change from entry 6</i>		
7	no photocatalyst	0
8	no base	2
9	no TRIP-SH	1
10	no light	0

^a Optimization reactions were performed on 0.05 mmol scale. Yields were determined by ¹H-NMR analysis of crude reaction mixtures relative to an internal standard.

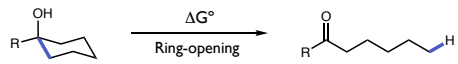
With these optimized conditions established, we next evaluated the scope of this isomerization protocol. Given the success of model substrate **1**, we were pleased to find that numerous other hexose and pentose derivatives were successful substrates, yielding linear formate products bearing complex arrays of protected polyols (Table 2, 2–5).

Table 2. Substrate Scope^a

^a Reactions run on 0.5 mmol scale. Reported yields are for isolated and purified material unless otherwise noted and are the average of two experiments. ^b GC yield reported relative to internal standard due to volatility. ^c PBU₄⁺(PhO)₂POO⁻ was the base. ^d PhCF₃ was the solvent. ^e CH₂Cl₂ was the solvent. ^f Tetrabutylphosphonium 5,5-dimethyl-1,3,2-dioxaphosphinan-2-olate 2-oxide (see SI for structure) was the base. ^g Reactions run on 2.0 mmol scale at 0.2 M. See SI for details.

Next, we turned our attention to simpler aliphatic alcohols. By examining a series of 2-methyl-substituted cyclic alcohols, we found that carbocycles of varying ring sizes could be opened efficiently (6–9). Various functional groups adjacent to the reactive hydroxyl groups were also well tolerated, including 2-phenyl, 2-NHBoc, 2-OTBS, 2-pyrazolyl, and spiro[4.5] substrates (10–14). Similarly, heteroatom substituents could also be incorporated into the ring structure (15, 16). A variety of more complex polycyclic structures could also be cleaved regioselectively, including derivatives of cholesterol, epiandrosterone, betulin, sclareolide, cedrol, isoborneol, and the Hajos-Parrish ketone (17–24). Interestingly, while substrate 19 contains two unprotected secondary alcohols, this protocol enables cleavage of the five-membered D-ring with >20:1 site-selectivity. In addition to the isomerization of cyclic alcohols, these reaction conditions enable the cleavage of carbon-substituents from acyclic alcohols, including various allyl-, benzyl-, and α -heteroatom-bearing carbon radical fragments (25–31). Furthermore, the model substrate from our previous report, a tertiary alcohol with a *p*-methoxyphenyl group (PMP), was isomerized smoothly (32), attesting to the generality of the new protocol. Last, we found that common model substrates for lignin degradation could also be processed using this protocol, breaking the central C–C bond to generate both the aldehyde and the alkoxybenzene products in good yields (33, 34).¹⁵ Notably, while the benzylic alcohol in 34 is cleaved first, the primary alcohol product 34b can undergo further cleavage under the reaction conditions, though this process is less efficient. During these scope studies, we found that the efficiency of this reaction is particularly sensitive to both the structure of the phosphate and the solvent, and beneficial deviations from the

Table 3. Computed Isomerization Thermochemistry of Selected Substrates



Substrate	Yield	ΔG° (kcal/mol) ^a
6	84%	+2.8
7	75%	+8.2
14	76%	+7.4
10	59%	+7.3
11	53% ^b	+12.7
12	71% ^c	+8.6
13	62%	+10.5
15	91% ^c	+6.6
16	81% ^c	+3.2
23	83%	+0.4
26	73% ^c	+4.3

^a All stationary point geometries and their corresponding energies were calculated using CBS-QB3 in gas phase. See SI for details. ^b Yield of TBS product. ^c Yield of *N*-Boc product.

optimal conditions are listed in the footnotes to Table 2. Also, we note that the use of toluene-*d*₈ solvent does not result in observable deuterium incorporation.

Computational evaluation of the thermochemistry (CBS-QB3) for numerous reactions in Table 2 revealed that the acyclic ring-opened carbonyl products are often significantly higher in energy than the cyclic alcohol starting materials (Table 3). However, as noted above, these catalytic reactions are redox-neutral isomerizations that consume no stoichiometric reagents other than photons. To account for these observations, we consider the elementary steps involved in the isomerization of alcohol 7 to aldehyde 7a in greater detail (Figure 3). In this figure, the various ensembles of 7, 7a, Ir photocatalyst, phosphate base, and thiol H-atom donor that are accessed along the reaction coordinate are designated as states A–G. Within this series, only states A and F are closed-shell singlet ground states, while all the others are open-shell states that exhibit triplet (or diradical) character. First, we observed no spectral overlap between the emission of the blue LEDs used in this study and the absorption profile of 7, ruling out direct excitation pathways. Similarly, the excited state of Ir is not quenched by 7 alone, discounting the possibility of triplet sensitization mechanisms. Instead, we propose that following photon absorption by the Ir(III) chromophore (A to B), the reaction commences with PCET activation of the O–H bond in 7 to furnish a key alkoxy radical intermediate (B to C).⁹ This intermediate can then either revert back to the initial state via charge recombination with the reduced Ir(II) state of the photocatalyst (C to A)¹⁶ or proceed forward through the β -scission and hydrogen atom transfer (HAT) steps *en route* to product (C to D to E to F). Importantly, the partitioning of C between these two pathways is kinetically controlled, and decoupled from the difference in the ground state energies of 7 and 7a.⁵

While this provides a means to access the higher energy isomer 7a, specific features of the reaction coordinate illustrated in Figure 3 also suggest a mechanism for maintenance of the resulting out-of-equilibrium state. In the forward direction, reduction of the alkyl radical intermediate by the aryl thiol (D to E) to form product 7a is significantly exergonic ($\Delta G^\circ = -18$ kcal/mol)¹⁷ and effectively irreversible when coupled to the subsequent charge recombination between the thiyl radical and the reduced Ir(II) state of the photocatalyst (E to F, $\Delta G^\circ = -32$ kcal/mol). This kinetic partitioning of E also precludes the viability of a light-driven reverse reaction to regenerate 7 from 7a. While E can likely be regenerated in an excited-state S–H PCET process from the aryl thiol (F to G to E)¹⁸, the requisite C–H HAT step necessary to traverse back to D is expected to be too slow ($\Delta G^\ddagger > +18$ kcal/mol) to compete kinetically with charge recombination between the thiyl and the reduced Ir(II) state of the photocatalyst, which will drive the system back to product state F.

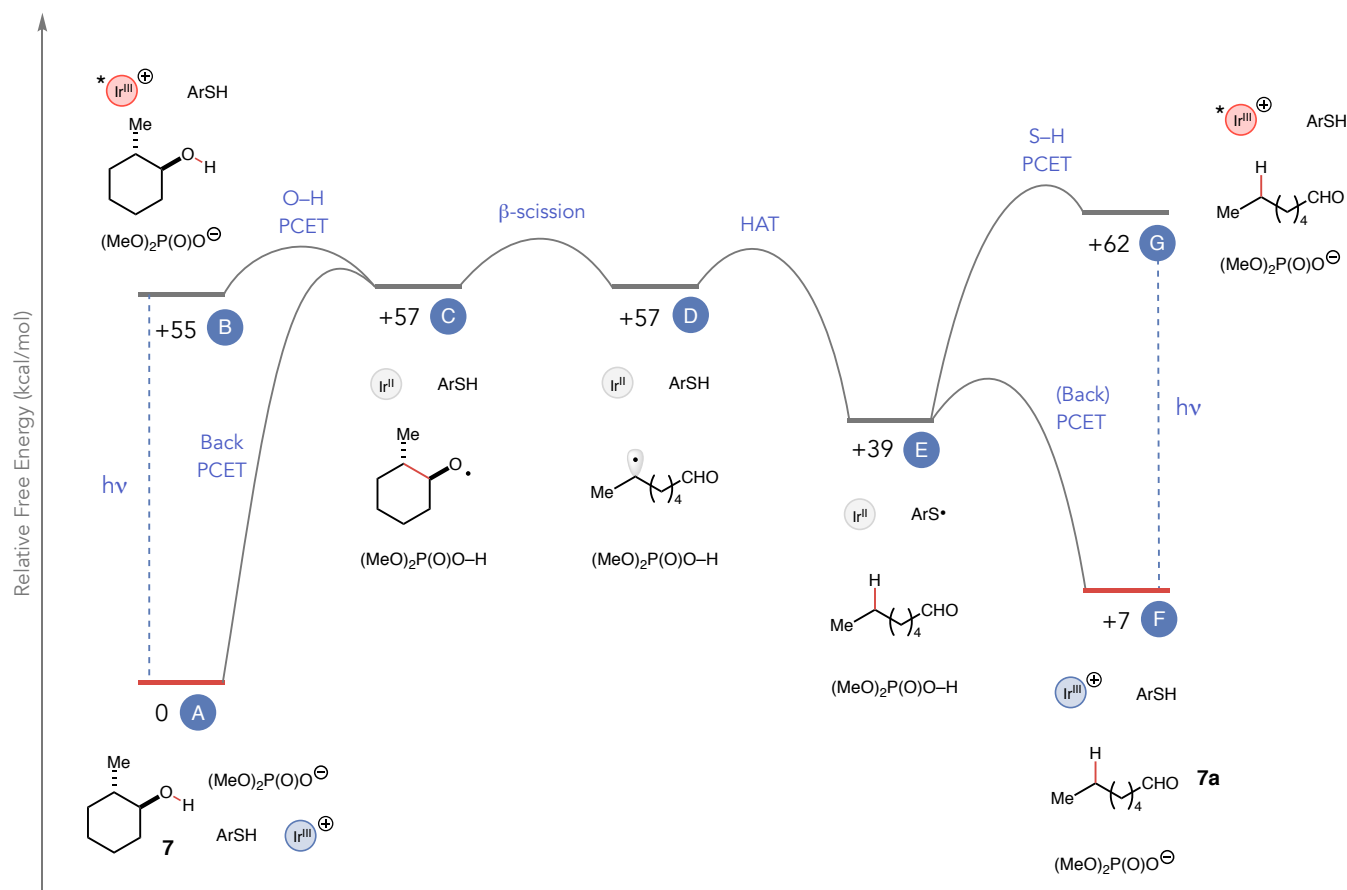


Figure 3. Proposed free energy profile for the contrathermodynamic isomerization of **7** to **7a**. The energy differences between states were estimated as follows: (a) (A to B & F to G) from 10% maxima of emission spectrum of **Ir** (524 nm); (b) (B to C) difference between cyclohexanol O–H BDFE and effective BDFE of photocatalyst **Ir** and tetrabutylammonium dimethyl phosphate (105 – 103 kcal/mol); (c) (C to D) from CBS-QB3 calculations of the energies of the two radicals; (d) (D to E) difference between heptane 2-methylene C–H BDFE and 2,4,6-trimethylbenzenethiol S–H BDFE (80 – 98 kcal/mol); (e) (E to F) difference between the effective BDFE of photocatalyst **Ir(II)** and dimethyl phosphoric acid and 2,4,6-trimethylbenzenethiol S–H BDFE (48 – 80 kcal/mol). (f) The estimate for A to F provided by this scheme is in reasonable agreement with the computed thermochemical data for **7** and **7a** presented in Table 3. See SI for details.

In a broader context, the mechanism described above highlights several design principles for achieving contrathermodynamic transformations driven by excited-state redox events. In particular, these results reinforce the notion that excited-state redox events are capable of breaking detailed balance in a manner similar to direct excitation and energy transfer-based mechanisms, enabling non-Boltzmann product distributions that are not dependent on the differences in the thermodynamic stabilities of starting materials and products. Maintenance of any resulting non-equilibrium state can be achieved through ratchet-type mechanisms that exhibit kinetic asymmetry between the forward and reverse reaction pathways created by photoexcitation and charge recombination steps.⁷ While similar models have been used to rationalize out-of-equilibrium behavior in supramolecular chemistry,⁸ we would posit that these energetic issues and their impacts on reaction directionality are not often considered, or duly exploited in photoredox catalysis.^{4,19} Yet, we anticipate that if these strategies can be general-

ized, they may have significant practical impacts in synthesis by providing a mechanism for overcoming the thermodynamic constraints that require transformations to proceed only in a single direction. Efforts to further advance these ideas are ongoing in our laboratory and will be reported in due course.

ASSOCIATED CONTENT

Supporting Information. Experimental details, characterization data, spectral data, and computational results.

The Supporting Information is available free of charge on the ACS Publications website.

Supporting information (PDF)

AUTHOR INFORMATION

Corresponding Author

*rknowles@princeton.edu

Notes

The authors declare no competing financial interest.

ACKNOWLEDGMENT

Financial support was provided by the NIH (R01 GM113105). E.O. was supported by a postdoctoral fellowship from the JSPS. We thank Tehshik Yoon for helpful discussions.

REFERENCES

- (1) (a) Schneider, C.; Weise, C. F. Cope, Oxy-Cope and Anionic Oxy-Cope Rearrangements. *Comprehensive Organic Synthesis*, 2nd ed., Knochel, P.; Molander, G. A., Eds.; Elsevier: 2014; Vol. 5, 867. (b) Martin-Castro, A. M.; Tortosa, M. Claisen Rearrangements. *Comprehensive Organic Synthesis*, 2nd ed., Knochel, P.; Molander, G. A., Eds.; Elsevier: 2014; Vol. 5, 912.
- (2) For notable exceptions, see: (a) Alexeeva, M.; Enright, A.; Dawson, M. J.; Mahmoudian, M.; Turner, N. J. Deracemization of α -Methylbenzylamine Using an Enzyme Obtained by In Vitro Evolution. *Angew. Chem. Int. Ed.* **2002**, *41*, 3177; (b) Lackner, A. D.; Samant, A. V.; Toste, F. D. Single-Operation Deracemization of 3H-Indolines and Tetrahydroquinolines Enabled by Phase Separation. *J. Am. Chem. Soc.* **2013**, *135*, 14090; (c) Ji, Y.; Shi, L.; Chen, M.-W.; Feng, G.-S.; Zhou, Y.-G. Concise Redox Deracemization of Secondary and Tertiary Amines with a Tetrahydroisoquinoline Core via a Nonenzymatic Process. *J. Am. Chem. Soc.* **2015**, *137*, 10496.
- (3) (a) Hartley, G. S. The *Cis*-form of Azobenzene. *Nature*, **1937**, *140*, 281; (b) Bandara, H. M. D.; Burdette, S. C. Photoisomerization in different classes of azobenzene. *Chem. Soc. Rev.* **2012**, *41*, 1809; (c) Hammond, G. S.; Saltiel, J. Photosensitized *Cis-Trans* Isomerization of the Stilbenes. *J. Am. Chem. Soc.* **1962**, *84*, 4983; (d) Arai, T.; Sakuragi, H.; Tokumaru, K. Unusual Behaviour of β -*tert*-alkylstyrenes in Photosensitized *Cis-Trans* Isomerization. Structural Effects on Triplet Energy Transfer. *Chem. Lett.* **1980**, *9*, 261; (e) Klajn, R. Spiropyran-based dynamic materials. *Chem. Soc. Rev.* **2014**, *43*, 148; (f) Irie, M.; Mohri, M. Thermally irreversible photochromic systems. Reversible photocyclization of diarylethene derivatives. *J. Org. Chem.* **1988**, *53*, 803; (g) Irie, M. Diarylethenes for Memories and Switches. *Chem. Rev.* **2000**, *100*, 1685; (h) Irie, M.; Fukaminato, T.; Matsuda, K.; Kobatake, S. Photochromism of Diarylethene Molecules and Crystals: Memories, Switches, and Actuators. *Chem. Rev.* **2014**, *114*, 12174; (i) Kobayashi, T.; Saito, T.; Ohtani, H. Real-Time Spectroscopy of Transition States in Bacteriorhodopsin During Retinal Isomerization. *Nature* **2001** *414*, 531.
- (4) For recent examples of sensitized olefin isomerization using visible light photocatalysis, see: (a) Singh, K.; Staig, S. J.; Weaver, J. D. Facile Synthesis of *Z*-Alkenes via Uphill Catalysis. *J. Am. Chem. Soc.* **2014**, *136*, 5275; (b) Molloy, J. J.; Metternich, J. B.; Daniliuc, C. G.; Watson, A. J. B.; Gilmour, R. Contra Thermodynamic, Photocatalytic *E*→*Z* Isomerization of Styrenyl Boron Species: Vectors to Facilitate Exploration of Two-Dimensional Chemical Space. *Angew. Chem. Int. Ed.* **2018**, *57*, 3168; (c) Metternich, J. B.; Artiukhin, D. G.; Holland, M. C.; von Bremen-Kühne, M.; Neugebauer, J.; Gilmour, R. Photocatalytic *E* → *Z* Isomerization of Polarized Alkenes Inspired by the Visual Cycle: Mechanistic Dichotomy and Origin of Selectivity. *J. Org. Chem.* **2017**, *82*, 9955; (d) Metternich, J. B.; Gilmour, R. A. Bio-Inspired, Catalytic *E* → *Z* Isomerization of Activated Olefins. *J. Am. Chem. Soc.* **2015**, *137*, 11254.
- (5) For a recent discussion, see: (a) Kathan, M.; Hecht, S. Photoswitchable Molecules as Key Ingredients to Drive Systems

- Away from the Global Thermodynamic Minimum. *Chem. Soc. Rev.* **2017**, *46*, 5536. (b) Astumian, R. D. Optical vs. Chemical Driving for Molecular Machines. *Faraday Discuss.* **2016**, *195*, 583.
- (6) Musacchio, A. J.; Lainhart, B. C.; Zhang, X.; Naguib, S. G.; Sherwood, T. C.; Knowles, R. R. Catalytic intermolecular hydroaminations of unactivated olefins with secondary alkyl amines. *Science*, **2017**, *355*, 727.
- (7) (a) Pezzato, C.; Cheng, C.; Stoddart, J. F.; Astumian, R. D. Mastering the Non-Equilibrium Assembly and Operation of Molecular Machines. *Chem. Soc. Rev.* **2017**, *46*, 5491; (b) Cheng, C.; McGonigal, P. R.; Stoddart, J. F.; Astumian, R. D. Design and Synthesis of Nonequilibrium Systems. *ACS Nano*, **2015**, *9*, 8672; (c) Astumian, R. D. Thermodynamics and Kinetics of Molecular Motors. *Biophys. J.* **2010**, *98*, 2401. (d) Kay, E. R.; Leigh, D. A.; Zerbetto, F. Synthetic Molecular Motors and Mechanical Machines. *Angew. Chem. Int. Ed.* **2007**, *46*, 72.
- (8) (a) Carlone, A.; Goldup, S. M.; Lebrasseur, N.; Leigh, D. A.; Wilson, A. A Three-Compartment Chemically-Driven Molecular Information Ratchet. *J. Am. Chem. Soc.* **2012**, *134*, 8321; (b) Alvarez-Pérez, M.; Goldup, S. M.; Leigh, D. A.; Slawin, A. M. Z. A Chemically-Driven Molecular Information Ratchet. *J. Am. Chem. Soc.* **2008**, *130*, 1836; (c) Chatterjee, M. N.; Kay, E. R.; Leigh, D. A. Beyond Switches: Ratcheting a Particle Energetically Uphill with a Compartmentalized Molecular Machine. *J. Am. Chem. Soc.* **2006**, *128*, 4058; (d) Hernández, J. V.; Kay, E. R.; Leigh, D. A. A Reversible Synthetic Rotary Molecular Motor. *Science*, **2004**, *306*, 1532. (e) Guentner, M.; Schildhauer, M.; Thumser, S.; Mayer, P.; Stephenson, D.; Mayer, P. J.; Dube, H. Sunlight-Powered kHz Rotation of a Hemithioindigo-Based Molecular Motor. *Nat. Commun.* **2015**, *6*, 8406; (f) Greb, L.; Lehn, J.-M. Light-Driven Molecular Motors: Imines as Four-Step or Two-Step Unidirectional Rotors. *J. Am. Chem. Soc.* **2014**, *136*, 13114; (g) Li, H.; Cheng, C.; McGonigal, P. R.; Fahrenbach, A. C.; Frasconi, M.; Liu, W.-G.; Zhu, Z.; Zhao, Y.; Ke, C.; Lei, J.; Young, R. M.; Dyrar, S. M.; Co, D. T.; Yang, Y.-W.; Botros, Y. Y.; Goddard, W. A., III; Wasielewski, M. R.; Astumian, R. D.; Stoddart, J. F. Relative Unidirectional Translation in an Artificial Molecular Assembly Fueled by Light. *J. Am. Chem. Soc.* **2013**, *135*, 18609; (h) Geertsema, E. M.; van der Molen, S. J.; Martens, M.; Feringa, B. L. Optimizing Rotary Processes in Synthetic Molecular Motors. *Proc. Nat. Acad. Sci.* **2009**, *106*, 16919.
- (9) Yayla, H. G.; Wang, H.; Tarantino, K. T.; Orbe, H. S.; Knowles, R. R. Catalytic Ring-Opening of Cyclic Alcohols Enabled by PCET Activation of Strong O–H Bonds. *J. Am. Chem. Soc.* **2016**, *138*, 10794.
- (10) For recent advances in catalytic β -scission chemistry: (a) Chiba, S.; Cao, Z.; El Bialy, S. A. A.; Narasaka, K. Generation of β -Keto Radicals from Cyclopropanols Catalyzed by AgNO₃. *Chem. Lett.* **2006**, *35*, 18; (b) Zhao, H.; Fan, X.; Yu, J.; Zhu, C. Silver-Catalyzed Ring-Opening Strategy for the Synthesis of β - and γ -Fluorinated Ketones. *J. Am. Chem. Soc.* **2015**, *137*, 3490; (c) Ren, R.; Zhao, H.; Huan, L.; Zhu, C. Manganese-Catalyzed Oxidative Azidation of Cyclobutanols: Regiospecific Synthesis of Alkyl Azides by C–C Bond Cleavage. *Angew. Chem. Int. Ed.* **2015**, *54*, 12692; (d) Ren, R.; Wu, Z.; Xu, Y.; Zhu, C. C–C Bond-Forming Strategy by Manganese-Catalyzed Oxidative Ring-Opening Cyanation and Ethynylation of Cyclobutanol Derivatives. *Angew. Chem. Int. Ed.* **2016**, *55*, 2866; (e) Guo, J.-J.; Hu, A.; Chen, Y.; Sun, J.; Tang, H.; Zuo, Z. Photocatalytic C–C Bond Cleavage and Amination of Cycloalkanols by Cerium(III) Chloride Complex. *Angew. Chem. Int. Ed.* **2016**, *55*, 15319; (f) Jia, K.; Zhang, F.; Huang, H.; Chen, Y. Visible-Light-Induced Alkoxy Radical Generation Enables Selective C(sp³)–C(sp³) Bond Cleavage and Functionalizations. *J. Am. Chem. Soc.* **2016**, *138*, 1514; (g) Jia, K.; Pan, Y.; Chen, Y. Selective Carbonyl–C(sp³) Bond Cleavage To Construct Ynamides, Ynoates, and Ynones by Pho-

- toredox Catalysis. *Angew. Chem. Int. Ed.* **2017**, *56*, 2478; (h) Hu, A.; Chen, Y.; Guo, J.-J.; Yu, N.; An, Q.; Zuo, Z. Cerium-Catalyzed Formal Cycloaddition of Cycloalkanols with Alkenes through Dual Photoexcitation. *J. Am. Chem. Soc.* **2018**, *140*, 13580; (i) Wu, X.; Wang, M.; Huan, L.; Wang, D.; Wang, J.; Zhu, C.; Tertiary-Alcohol-Directed Functionalization of Remote C(sp³)-H Bonds by Sequential Hydrogen Atom and Heteroaryl Migrations. *Angew. Chem. Int. Ed.* **2018**, *57*, 1640; (j) Guo, J.-J.; Hu, A.; Zuo, Z. Photocatalytic alkoxy radical-mediated transformations. *Tet. Lett.* **2018**, *59*, 2103. (k) Wang, D.; Mao, J.; Zhu, C. Visible light-promoted ring-opening functionalization of unstrained cycloalkanols via inert C-C bond scission. *Chem. Sci.* **2018**, *9*, 5805; (l) Roque, J. B.; Kuroda, Y.; Göttemann, L. T.; Sarpong, R. Deconstructive fluorination of cyclic amines by carbon-carbon cleavage. *Science*, **2018**, *361*, 171.
- (11) (a) Baciocchi, E.; Bietti, M.; Lanzalunga, O. Mechanistic Aspects of β -Bond-Cleavage Reactions of Aromatic Radical Cations. *Acc. Chem. Res.* **2000**, *33*, 243; (b) Baciocchi, E.; Bietti, M.; Lanzalunga, O.; Steenken, S. Oxygen Acidity of 1-Arylalkanol Radical Cations. 4-Methoxycumyloxy Radical as $-C(Me)_2-O^-$ -to-Nucleus Electron-Transfer Intermediate in the Reaction of 4-Methoxycumyl Alcohol Radical Cation with OH \cdot . *J. Am. Chem. Soc.* **1998**, *120*, 11516.
- (12) For general PCET references, see: (a) Reece, S. Y.; Nocera, D. G. Proton-Coupled Electron Transfer in Biology: Results from Synergistic Studies in Natural and Model Systems. *Annu. Rev. Biochem.* **2009**, *78*, 673; (b) Warren, J. J.; Tronic, T. A.; Mayer, J. M. Thermochemistry of Proton-Coupled Electron Transfer Reagents and its Implications. *Chem. Rev.* **2010**, *110*, 6961; (c) Weinberg, D. R.; Gagliardi, C. J.; Hull, J. F.; Murphy, C. F.; Kent, C. A.; Westlake, B. C.; Paul, A.; Ess, D. H.; McCafferty, D. G.; Meyer, T. J. Proton-Coupled Electron Transfer. *Chem. Rev.* **2012**, *112*, 4016; (d) Miller, D. C.; Tarantino, K. T.; Knowles, R. R. Proton-Coupled Electron Transfer in Organic Synthesis: Fundamentals, Applications, and Opportunities. *Top. Curr. Chem.* **2016**, *374*, 145.
- (13) For other synthetic examples utilizing oxidative PCET, see: (a) Choi, G. J.; Knowles, R. R. Catalytic Alkene Carboaminations Enabled by Oxidative Proton-Coupled Electron Transfer. *J. Am. Chem. Soc.* **2015**, *137*, 9226; (b) Miller, D. C.; Choi, G. J.; Orbe, H. S.; Knowles, R. R. Catalytic Olefin Hydroamidation Enabled by Proton-Coupled Electron Transfer. *J. Am. Chem. Soc.* **2015**, *137*, 13492; (c) Choi, G. J.; Zhu, Q.; Miller, D. C.; Gu, C. J.; Knowles, R. R. Catalytic alkylation of remote C-H bonds enabled by proton-coupled electron transfer. *Nature*, **2016**, *539*, 268; (d) Zhu, Q.; Graff, D. E.; Knowles, R. R. Intermolecular Anti-Markovnikov Hydroamination of Unactivated Alkenes with Sulfonamides Enabled by Proton-Coupled Electron Transfer. *J. Am. Chem. Soc.* **2018**, *140*, 741; (e) Gentry, E. C.; Rono, L. J.; Hale, M. E.; Matsuura, R.; Knowles, R. R. Enantioselective Synthesis of Pyrroloindolines via Noncovalent Stabilization of Indole Radical Cations and Applications to the Synthesis of Alkaloid Natural Products. *J. Am. Chem. Soc.* **2018**, *140*, 3394.
- (14) (a) Wohl, A. Abbau des Traubenzuckers. *Chem. Ber.* **1893**, *26*, 730; (b) de Armas, P.; Francisco, C. G.; Suarez, E. Reagents with Hypervalent Iodine: Formation of Convenient Chiral Synthetic Intermediates by Fragmentation of Carbohydrate Anomeric Alkoxy Radicals. *Angew. Chem. Int. Ed.* **1992**, *31*, 772; (c) de Armas, P.; Francisco, C. G.; Suarez, E. Fragmentation of carbohydrate anomeric alkoxy radicals. Tandem β -fragmentation-cyclization of alcohols. *J. Am. Chem. Soc.* **1993**, *115*, 8865.
- (15) (a) Yang, L.; Seshan, K.; Li, Y. A review on thermal chemical reactions of lignin model compounds. *Catal. Today*, **2017**, *298*, 276; (b) Bosque, I.; Magallanes, G.; Rigoulet, M.; Kärkäs, M. D.; Stephenson, C. R. J. Redox Catalysis Facilitates Lignin Depolymerization. *ACS Cent. Sci.* **2017**, *3*, 621; (c) Son, S.; Toste, F. D. Non-Oxidative Vanadium-Catalyzed C-O Bond Cleavage: Application to Degradation of Lignin Model Compounds. *Angew. Chem. Int. Ed.* **2010**, *49*, 3791.
- (16) For discussion of charge recombination in photocatalysis, see: (a) Ruccolo, S.; Qin, Y.; Schnedermann, C.; Nocera, D. G. General Strategy for Improving the Quantum Efficiency of Photo-redox Hydroamidation Catalysis. *J. Am. Chem. Soc.* **2018**, *140*, 14926; (b) Gould, I. R.; Farid, S. Dynamics of Bimolecular Photoinduced Electron-Transfer Reactions. *Acc. Chem. Res.* **1996**, *29*, 522.
- (17) See SI for calculation details. The BDEs of C-H and S-H bonds are from: Luo, Y.-R. *Comprehensive Handbook of Chemical Bond Energies*; CRC Press: Boca Raton, FL, 2007.
- (18) (a) Gagliardi, C. J.; Murphy, C. F.; Binstead, R. A.; Thorp, H. H.; Meyer, T. J. Concerted Electron-Proton Transfer (EPT) in the Oxidation of Cysteine. *J. Phys. Chem. C*, **2015**, *119*, 7028; (b) Kuss-Petermann, M.; Wenger, O. S. Mechanistic Diversity in Proton-Coupled Electron Transfer between Thiophenols and Photoexcited $[Ru(2,2'-Bipyrazine)_3]^{2+}$. *J. Phys. Chem. Lett.* **2013**, *4*, 2535.
- (19) Selected examples of photocatalytic reactions with non-equilibrium outcomes: (a) West, J. G.; Huang, D.; Sorensen, E. J. Acceptorless dehydrogenation of small molecules through cooperative base metal catalysis. *Nat. Commun.* **2015**, *6*, 10093; (b) Abrams, D. J.; West, J. G.; Sorensen, E. J. Toward a mild dehydroformylation using base-metal catalysis. *Chem. Sci.*, **2017**, *8*, 1954; (c) Lehnher, D.; Ji, Y.; Neel, A. J.; Cohen, R. D.; Brunskill, A. P. J.; Yang, J.; Reibarkh, M. Discovery of a Photoinduced Dark Catalytic Cycle Using *in Situ* LED-NMR Spectroscopy. *J. Am. Chem. Soc.* **2018**, *140*, 13843.

